

Electrically-Active Convection in Tropical Easterly Waves and Implications for Tropical Cyclogenesis in the Atlantic and East Pacific

K. Leppert II, Dept. Atmospheric Science, University of Alabama in Huntsville

W. Petersen, NASA GSFC/WFF (walt.petersen@nasa.gov)

D. Cecil, Earth Systems Sciences Center, University of Alabama in Huntsville

One possible key to improving tropical cyclone initiation forecasting is to understand how a given tropical wave disturbance acts to organize areas of deep convection and precipitation that form the “seeds” of incipient tropical storms and/or hurricanes. Because on average only one in ten tropical waves tend to develop tropical cyclones, it is beneficial to be able to recognize clues that suggest eventual intensification of any given wave. Related questions would be: Can satellite remote sensing tools be used to identify incipient cyclone “seeds” of intensification within a given tropical wave? More specifically, can the observed strength and evolution of deep convective storms and precipitation typically observed in tropical disturbances be used as a metric for indications of future tropical cyclone development?

To answer the aforementioned questions, in this study we investigate the evolution of individual convective storm structures within tropical easterly waves across the Atlantic and Eastern Pacific Ocean Basins. We examine diagnostics of convective storm intensity (infrared cloud top temperatures, lightning, and microwave brightness temperatures) as a function of the surrounding environment (e.g., large scale mass and moisture convergence profiles in the disturbances) as a means to assess the mechanisms by which convective storms might influence cyclone development and the potential role/use of convective storm intensity observations for predicting tropical cyclogenesis. We use data from the Tropical Rainfall Measurement Mission (TRMM) satellite Microwave Imager (TMI), Precipitation Radar (PR), and Lightning Imaging Sensor (LIS) as well as infrared (IR) brightness temperature data from the NASA global-merged IR brightness temperature dataset to evaluate convective storm intensities within given easterly waves across the Atlantic and Pacific regions of study and how those intensity diagnostics differ between tropical easterly waves that do or do not spawn tropical cyclones

The study results suggest that convective storm intensity diagnostics that best distinguish developing from non-developing cyclone waves vary as a function of where a given wave actually spawns a tropical cyclone. For waves that develop cyclones in the Atlantic basin, coverage by IR brightness temperatures less than 240 K and 210 K seems to provide the best distinction between developing and non-developing waves. Over the East Pacific several variables seem to provide a significant distinction between cyclone-developing and non-developing waves. These variables include the same IR temperature coverage thresholds as observed in the Atlantic Basin, in addition to lightning flash rate, and low-level (<4.5 km) PR reflectivity which are all increased in the convection of easterly waves that develop cyclones. The results of this study are consistent with previously hypothesized feedbacks between wave convective structures and tropical cyclogenesis, and also reasonably suggest that satellite remote sensing diagnostics that discern the intensity of storm clusters within tropical disturbances may provide some guidance for distinguishing waves that are or are not likely to develop tropical cyclones.

Monthly Weather Review

Electrically-Active Convection in Tropical Easterly Waves and Implications for Tropical Cyclogenesis in the Atlantic and East Pacific --Manuscript Draft--

Manuscript Number:	
Full Title:	Electrically-Active Convection in Tropical Easterly Waves and Implications for Tropical Cyclogenesis in the Atlantic and East Pacific
Article Type:	Article
Corresponding Author:	Kenneth David Leppert II University of Alabama in Huntsville Huntsville, AL UNITED STATES
Corresponding Author's Institution:	University of Alabama in Huntsville
First Author:	Kenneth David Leppert II
Order of Authors:	Kenneth David Leppert II Walter Petersen Daniel Cecil
Abstract:	<p>In this study, we investigate the characteristics of tropical easterly wave convection and the possible implications of convective structure on tropical cyclogenesis and intensification over the Atlantic Ocean and East Pacific using data from the Tropical Rainfall Measurement Mission Microwave Imager, Precipitation Radar (PR), and Lightning Imaging Sensor as well as infrared (IR) brightness temperature data from the NASA global-merged IR brightness temperature dataset.</p> <p>Easterly waves were partitioned into northerly, southerly, trough, and ridge phases based on the 700-hPa meridional wind from the NCEP-NCAR reanalysis dataset. Waves were subsequently divided according to whether they did or did not develop tropical cyclones (i.e., developing and nondeveloping, respectively), and developing waves were further subdivided according to development location. Finally, composites as a function of wave phase and category were created using the various datasets.</p> <p>Results suggest that the convective characteristics that best distinguish developing from nondeveloping waves vary according to where developing waves spawn tropical cyclones. For waves that developed a cyclone in the Atlantic basin, coverage by IR brightness temperatures ≤ 240 K and ≤ 210 K provide the best distinction between developing and nondeveloping waves. In contrast, several variables provide a significant distinction between nondeveloping waves and waves that develop cyclones over the East Pacific as these waves near their genesis location including IR threshold coverage, lightning flash rates, and low-level (<4.5 km) PR reflectivity. Results of this study may be used to help develop thresholds to better distinguish developing from nondeveloping waves and serve as another aid for tropical cyclogenesis forecasting.</p>
Suggested Reviewers:	

1
2
3
4
5
6
7
8
9
10
11
12
13
14
15
16
17
18
19
20
21
22
23

**Electrically-Active Convection in Tropical Easterly Waves and Implications
for Tropical Cyclogenesis in the Atlantic and East Pacific**

Kenneth D. Leppert II*
Walter A. Petersen+
and
Daniel J. Cecil*

*University of Alabama Huntsville, Huntsville, Alabama

+NASA GSFC/Wallops Flight Facility Code 610.W, Wallops Island, Virginia

SUBMITTED TO *MONTHLY WEATHER REVIEW* 15 June 2012

*Corresponding author address: Kenneth Leppert II, NSSTC, 320 Sparkman Dr Rm 4074, Huntsville, AL
35805
E-mail: leppert@nsstc.uah.edu

24 ABSTRACT

25 In this study, we investigate the characteristics of tropical easterly wave convection and
26 the possible implications of convective structure on tropical cyclogenesis and intensification over
27 the Atlantic Ocean and East Pacific using data from the Tropical Rainfall Measurement Mission
28 Microwave Imager, Precipitation Radar (PR), and Lightning Imaging Sensor as well as infrared
29 (IR) brightness temperature data from the NASA global-merged IR brightness temperature
30 dataset.

31 Easterly waves were partitioned into northerly, southerly, trough, and ridge phases based
32 on the 700-hPa meridional wind from the NCEP-NCAR reanalysis dataset. Waves were
33 subsequently divided according to whether they did or did not develop tropical cyclones (i.e.,
34 developing and nondeveloping, respectively), and developing waves were further subdivided
35 according to development location. Finally, composites as a function of wave phase and
36 category were created using the various datasets.

37 Results suggest that the convective characteristics that best distinguish developing from
38 nondeveloping waves vary according to where developing waves spawn tropical cyclones. For
39 waves that developed a cyclone in the Atlantic basin, coverage by IR brightness temperatures
40 ≤ 240 K and ≤ 210 K provide the best distinction between developing and nondeveloping waves.
41 In contrast, several variables provide a significant distinction between nondeveloping waves and
42 waves that develop cyclones over the East Pacific as these waves near their genesis location
43 including IR threshold coverage, lightning flash rates, and low-level (< 4.5 km) PR reflectivity.
44 Results of this study may be used to help develop thresholds to better distinguish developing
45 from nondeveloping waves and serve as another aid for tropical cyclogenesis forecasting.

47 **1. Introduction**

48
49

50 African easterly waves (AEWs) form in the tropical easterlies over east-central Africa
51 (e.g., Burpee 1972; Norquist et al. 1977; Reed et al. 1977; Berry and Thorncroft 2005;
52 Thorncroft et al. 2008) and often form the necessary precursor low-level disturbance for tropical
53 cyclogenesis (Kurihara and Tuleya 1981). These waves are important for tropical cyclogenesis
54 not only in the Atlantic (e.g., Landsea 1993), but also in the East Pacific (e.g., Avila 1991; Avila
55 and Pasch 1992; Molinari and Vollaro 2000; note, however, that not all easterly waves found
56 over the East Pacific originate over Africa; e.g., Serra et al. 2008, 2010).

57 One outstanding question is why some waves develop tropical cyclones while others do
58 not. Many factors that play a role in determining whether a wave develops involve the
59 environment through which an easterly wave propagates. For example, a wave may be more
60 likely to develop a tropical cyclone if it propagates through a region of weak vertical wind shear,
61 SSTs $>27^{\circ}\text{C}$, below-average sea-level pressure, above-normal low-level relative vorticity, and/or
62 above-average precipitable water (all conditions favorable for tropical cyclogenesis; e.g., Gray
63 1968; Landsea et al. 1998; Bracken and Bosart 2000).

64 Hopsch et al. (2010) suggest that the structure of AEWs near the West African coast may
65 be another important influence for determining the likelihood of cyclone development. In that
66 study, developing waves were associated with higher values of relative humidity as well as
67 stronger mid- and low-level circulations compared to nondeveloping waves (NDWs). In
68 addition, it was found that developing waves tend to undergo a transformation from a cold-core
69 structure over the African continent to a warm-core structure at the coast and over the ocean,
70 consistent with cyclogenesis, while NDWs showed no such transformation. Results of Hopsch et

71 al. (2010) also indicated that differences in the structure of developing waves and NDWs at the
72 coast could influence the likelihood of development out to 60°W over the Atlantic Ocean.

73 Easterly waves are often associated with convection at some point in their lifetime (e.g.,
74 Burpee 1974; Thompson et al. 1979; Duvel 1990; Petersen et al. 2003; Petersen and Boccippio
75 2004; Leppert and Petersen 2010; hereafter LP10), and differences in the nature of this
76 convection between different waves may be another determinant for why some waves develop
77 while others do not. Via thermodynamic and dynamic feedbacks between the smaller convective
78 scale and larger synoptic scale, more intense and/or widespread convection associated with
79 developing waves could help to produce conditions in the wave more favorable for development.

80 One possible effect of convection on the larger scale favorable for tropical cyclogenesis
81 is an increase in mid- to low-level vorticity. Ritchie and Holland (1997) showed how many
82 midlevel, convective-scale vortices created by convection can interact and merge, resulting in
83 one larger, cyclonic circulation (i.e., mesoscale convective vortex), helping to increase midlevel
84 vorticity on a larger scale. Hendricks et al. (2004) and Montgomery et al. (2006) used numerical
85 model simulations to describe a similar process near the surface whereby convection can help to
86 increase low-level vorticity and aid cyclogenesis. In particular, intense convective towers (i.e.,
87 vortical hot towers) were found to acquire large values of vertical vorticity via the tilting and
88 stretching of preexisting vorticity by convective updrafts. Montgomery et al. (2006) suggest that
89 a population of many growing, merging, and decaying towers acts as a quasi-steady diabatic
90 heating rate which feeds back to the large-scale circulation. In order for the circulation to remain
91 in thermal wind balance a secondary radial circulation develops with inflow near the surface.
92 This near-surface inflow encourages vortex merger, the concentration of low-level vorticity, and
93 the intensification of the cyclone (Hendricks et al. 2004; Montgomery et al. 2006). Several

94 observation-based studies have also provided evidence for the importance of hot towers for
95 increasing low-level vorticity and aiding tropical cyclogenesis (e.g., Reasor et al. 2005; Sippel et
96 al. 2006; Houze et al. 2009).

97 Another potential contribution of persistent, widespread convection to the genesis process
98 is the moistening of mid and upper levels via transport of moisture from the surface. In
99 particular, Dunkerton et al. (2009) emphasizes the importance for tropical cyclogenesis of the
100 containment and accumulation of moisture transported by convection within a Lagrangian re-
101 circulation region of the trough phase of an easterly wave. This moisture transport and/or
102 accumulation inhibits the development of evaporatively-cooled downdrafts and associated
103 transport of low equivalent potential temperatures to the surface, which is thought to inhibit
104 tropical cyclogenesis (Rotunno and Emanuel 1987). Nolan (2007) also showed the importance
105 of mid- and upper-level moistening for tropical cyclogenesis.

106 Because enhanced convection could potentially enhance the development of an easterly
107 wave circulation and structure more favorable for tropical cyclogenesis, it is not surprising that
108 previous studies have found developing waves to be associated with more intense and/or
109 widespread convection compared to NDWs. For example, Hopsch et al. (2010) used IR
110 brightness temperatures to determine that developing waves are, in fact, associated with more
111 widespread/intense convection. Chronis et al. (2007) used lightning frequency to infer the
112 intensity of convection and found that tropical cyclogenesis in the East Atlantic may be related to
113 enhanced electrical activity (i.e., more intense convection) over that region. In this case,
114 lightning represents a proxy for deep convective updrafts and robust mixed-phase microphysical
115 processes, previously demonstrated to be a prerequisite for the development of strong in-cloud
116 electric fields and associated lightning (e.g., Takahashi 1978; Rutledge et al. 1992; Williams et

117 al. 1992; Zipser 1994; Saunders and Peck 1998; Deierling and Petersen 2008). In addition, Price
118 et al. (2007) showed that enhanced lightning over East Africa may also be associated with
119 cyclogenesis over the East Atlantic. Leary and Ritchie (2009) examined cloud clusters instead of
120 waves in the East Pacific and found that developing cloud clusters were associated with
121 significantly more lightning than nondeveloping clusters. LP10 examined IR brightness
122 temperatures as well as lightning associated with AEWs over several longitude bands stretching
123 from East Africa (30°E) to the central Atlantic (50°W). They found that over each longitude
124 band developing waves were associated with a greater coverage of more intense, electrically-
125 active convection compared to NDWs.

126 This study expands on previous studies by not only examining lightning and/or IR
127 brightness temperatures for clues about convection related to tropical cyclogenesis but also
128 examining microwave brightness temperatures from the Tropical Rainfall Measurement Mission
129 (TRMM) Microwave Imager (TMI) and radar reflectivity data from the TRMM Precipitation
130 Radar (PR). In particular, the purpose of this study is twofold: 1.) Determine which
131 observations/characteristics of convection provide the best distinction between developing waves
132 and NDWs. 2.) Determine whether the characteristics that provide the best distinction vary for
133 waves that develop tropical cyclones over different regions. This paper composites all easterly
134 wave observations over fixed regions (i.e., Eulerian framework), while a companion study
135 (Leppert and Cecil 2012) examines composites in a wave-following, Lagrangian sense. The
136 Eulerian methodology and the associated results from this paper could potentially be used to help
137 distinguish developing waves from NDWs for forecasting applications. In contrast, the
138 Lagrangian methodology used in Leppert and Cecil (2012) requires a priori information
139 describing when and where a wave developed a tropical cyclone, limiting its direct application to

140 the forecasting process. But, the Lagrangian framework can provide information on the
141 evolution of waves in the days leading up to cyclogenesis (i.e., a greater understanding of the
142 genesis process) that cannot be obtained from the Eulerian approach.

143 144 **2. Data/Methodology**

145
146
147 Following the methodology of LP10, we analyzed easterly waves by partitioning the
148 waves into phases (ridge, northerly, trough, and southerly phases) based on NCEP-NCAR
149 reanalysis (Kalnay et al. 1996) 700-hPa meridional wind data (note that the reanalysis has a
150 spatial [temporal] resolution of 2.5° [six hours; averaged to one day for this study]).
151 Specifically, the various wave phases were identified by first calculating a daily average
152 meridional wind value between 5°–20°N and then calculating a meridional wind anomaly
153 (relative to the mean at each longitude) for each day and longitude. Next, a 3–7 day bandpass
154 filter was applied to the anomalies in order to isolate the period of the easterly waves. The
155 filtered anomalies were subsequently normalized by the standard deviation valid at each
156 longitude, and the ± 0.75 standard deviation threshold was used to identify the individual wave
157 phases. In particular, normalized anomalies greater (less) than 0.75 (-0.75) were classified as the
158 southerly (northerly) phase. For a given day, values between northerly (southerly) and southerly
159 (northerly) phases were identified as trough (ridge) phases. Finally, to classify many of those
160 data points unable to be classified using meridional wind data alone, 700-hPa vorticity was
161 calculated using reanalysis zonal and meridional wind components and processed exactly as the
162 meridional wind data.

163 The analysis domain over which the wave phases were identified for this study was larger
164 than that used in LP10 and stretched from 130°W to 20°E and from 5°N to 20°N, outlined in Fig.

165 1. To examine the evolution of convection and cold cloudiness associated with the waves as
166 they propagated through our analysis domain, the full analysis domain was divided into five
167 longitude bands, also shown in Fig. 1. These bands stretched from 130°W to 95°W over the East
168 Pacific (EPC), from 95°W to 70°W over the Western Caribbean and far eastern Pacific region
169 (CAR; this band includes the Central American land mass as well as the northern part of South
170 America), from 70°W to 40°W over the West Atlantic (WAT), from 40°W to 15°W over the
171 East Atlantic (EAT; the eastern boundary of this band lies approximately along the West African
172 coast), and from 15°W to 20°E over Africa (AFR). The waves were analyzed for the months of
173 June–November for the 10-year span of 2001–2010. These are the months in which easterly
174 waves are the most pronounced (e.g., Carlson 1969; Gu et al. 2004) and when tropical cyclones
175 often develop in the Atlantic and East Pacific regions (National Hurricane Center [NHC] storm
176 reports; NHC 2011).

177 After the various wave phases were identified, the wave troughs were divided into
178 developing (i.e., waves that developed tropical cyclones that attained at least tropical storm
179 strength) and NDWs (i.e., waves that never developed a tropical cyclone; see Table 1 for
180 acronyms and definitions of each wave category used in this study) via information provided by
181 NHC (2011). In addition, developing waves were divided based on the longitude band over
182 which they developed a tropical depression. Once the trough phases were partitioned into
183 various categories, any of the other three wave phases found within three data points (7.5°) east
184 or west of each wave trough were considered to be part of that wave and used in the composites.

185 The Lightning Imaging Sensor (LIS) on board TRMM consists of an optical imager
186 capable of recording brief radiance events associated with lightning (Christian et al. 1992;
187 Boccippio et al. 2002) with an estimated detection efficiency of 70%–90% (Christian 1999;

188 Boccippio et al. 2000, 2002; no correction for detection efficiency was utilized for this study). In
189 particular, we used the 0.5° LIS flash counts and view time data to compute the daily lightning
190 flash density for 2.5° grid boxes (total flash count divided by view time over the area of a 2.5°
191 grid box).

192 The PR is a phased array radar system operating at 13.8 GHz (Kummerow et al. 1998;
193 Kozu et al. 2001). Specifically, attenuation-corrected radar reflectivity (Iguchi et al. 2000;
194 Meneghini et al. 2000; Iguchi et al. 2009) and a convective/stratiform classification (Awaka et al.
195 1998, 2009) from the PR 2A25 V6.0 product were utilized for this study. The reflectivity values
196 classified as convective were used to calculate mean convective reflectivity profiles for each 2.5°
197 box with 1-km height resolution from 1–18 km above ground level. Only convective rays of
198 data with a rain bottom below 2 km and not classified as warm rain were used in the construction
199 of these mean profiles to isolate the type of convection presumably most relevant for tropical
200 cyclogenesis.

201 The convective rain classification from 2A25 V6.0 was also used to tabulate the
202 percentage convective coverage over each 2.5° box. Another coverage parameter was calculated
203 using data from the 4-km NASA global-merged IR brightness temperature dataset (Liu et al.
204 2009). Specifically, the fractional coverage by IR brightness temperatures ≤ 210 K and ≤ 240 K
205 over each 2.5° box was calculated to examine the coverage by cold cloudiness.

206 The TMI instrument is a nine-channel passive microwave radiometer (Kummerow et al.
207 1998). Four TMI channels were used in this study, including the 37.0 GHz and 85.5 GHz
208 horizontally- and vertically-polarized channels. The measured radiances in these channels are
209 especially sensitive to scattering by ice (e.g., Spencer et al. 1989; Smith et al. 1992; Cecil and
210 Zipser 1999; Toracinta et al. 2002). Significant scattering and an accompanying reduction in the

211 measured brightness temperatures at 85.5 GHz can be accomplished by relatively small ice
212 particles ($\sim 10^{-4}$ m in diameter), but significant reductions in brightness temperatures at 37.0 GHz
213 require the presence of larger (millimeter-sized) particles (Toracinta et al. 2002). Therefore, a
214 significant reduction in 37.0-GHz brightness temperatures likely indicates a stronger updraft and
215 more intense convection required for the formation and maintenance of large ice particles in the
216 upper portions of clouds. The 85.5-GHz channel has also been used in several earlier studies to
217 characterize the intensity and spatial extent of convection (e.g., Mohr and Zipser 1996; Cecil and
218 Zipser 1999; Mohr et al. 1999).

219 At 37.0 and 85.5 GHz, variations in surface emissivity and temperature can lead to large
220 variations in brightness temperature unrelated to the overlying atmosphere. To remove these
221 variations, we combined temperatures measured from both 85.5-GHz channels into 85.5-GHz
222 polarization corrected temperatures (PCT_{85}) as defined by Spencer et al. (1989). Similarly, the
223 two 37.0-GHz channels were combined to form PCT_{37} as defined by Toracinta et al. (2002) and
224 Cecil et al. (2002). Cecil and Zipser (2002) found that vigorous convection was generally
225 present when PCT_{85} were below ~ 200 K and PCT_{37} were below ~ 263 K. Hence, only TMI
226 pixels with $PCT_{85} \leq 200$ K and $PCT_{37} \leq 260$ K were used to calculate an average PCT_{85} and
227 PCT_{37} over each 2.5° box.

228 Lightning flash rates, mean convective reflectivity profiles, mean PCTs, percentage
229 convective coverage values, and IR fractional coverage values were subsequently composited as
230 a function of wave phase for the different wave types over the various longitude bands (Fig. 1).
231 Note that some developing wave composites were not created over every longitude band because
232 after initial tropical cyclone development, developing waves were no longer tracked. For
233 example, composites were created for waves which spawn tropical cyclones over the East

234 Atlantic (i.e., East Atlantic developing waves; EADWs) over only the Africa and East Atlantic
235 longitude bands. EADWs were tracked up until they developed cyclones over the East Atlantic
236 but not farther west.

237 The parameters we analyze here basically relate to either the areal coverage of convection
238 (percentage convective coverage, coverage below IR brightness temperature thresholds) or the
239 vigor of convection that does occur (lightning flash rate, mean PCTs for pixels below certain
240 thresholds, mean convective reflectivity). The IR thresholds (210 K and 240 K) go beyond
241 characterizing the convective area as cold anvils expand. Flash rate is somewhat related to both
242 the coverage and intensity of convection, but one or more elements of intense convection can
243 dominate this parameter much more than a large number of weak convective cells would. The
244 PCT thresholds used here restrict the analysis to only pixels related to strong, deep convection.
245 Hence, our mean PCT values are indicative of how strong that convection is when it does occur.
246 (Note that taking the mean PCT without using thresholds [not shown] would be more related to
247 the rain area and would be quite different than the mean PCTs with thresholds.) Similarly, our
248 mean reflectivity values consider only the pixels that are already classified as convective, so they
249 relate to how strong that convection is.

250 In order to test whether values from developing waves and NDWs are significantly
251 different, the analysis of variance statistical technique was used. This provides an estimate of the
252 error variance associated with some group of data and an estimate of the systematic variance
253 between groups of data. If the systematic variance is greater than the error variance, then the f-
254 statistic is used to test whether the systematic effect is significantly greater than the random error
255 effect. A significantly greater systematic effect suggests a high probability that differences
256 between groups of data are, indeed, real and not just due to chance. Note for this study that a

257 difference is considered to be significant if the f-statistic indicates significance at or above the
258 99% level. Additional information on the analysis of variance technique can be found in
259 Panofsky and Brier (1958).

260 261 **3. Results**

262 263 264 *a. Comparison between East Atlantic Developing Waves and NDWs*

265
266
267 Table 2 shows the number of distinct easterly waves and the number of individual data
268 points included in the trough phase composites of various wave categories, including EADWs
269 and NDWs. Note that as a result of wave merger/splitting as well as the ambiguities associated
270 with counting weak NDWs that alternately can be tracked for a short time over the analysis
271 domain and then become too weak to be tracked, the number of distinct NDWs in Table 2 is only
272 an estimate.

273 The composite coverage by IR brightness temperature thresholds are provided in Table 3
274 over various longitude bands for various wave categories, including for EADWs and NDWs.
275 Over Africa, the coverage by temperatures ≤ 210 K and ≤ 240 K is significantly greater in all
276 EADW phases (except for the 210 K threshold in the trough phase) compared to the
277 corresponding NDW values. Over the East Atlantic, significantly greater EADW values are
278 confined to only the trough and northerly phases. Similarly, the composite percentage
279 convective coverage values for EADWs and NDWs in Table 4 indicate that coverage is greater
280 for EADWs over both Africa and the East Atlantic in each wave phase, except the ridge phase
281 over the East Atlantic. The differences between EADWs and NDWs in the northerly phase over
282 both Africa and the East Atlantic are significant, and the difference between trough phase values
283 over the East Atlantic is also relatively large (while not significant at the 99% level, it is

284 significant at the 95% level). Thus, as EADWs approach their genesis region over the East
285 Atlantic, the maximum convective and cold cloudiness coverage occurs ahead of and within the
286 wave trough where it may interact with the larger-scale wave helping to amplify the wave,
287 perhaps making it more favorable for cyclogenesis (LP10).

288 While the differences in composite lightning flash rates (Table 5) between EADWs and
289 NDWs over Africa are not significant at the 99% level, all EADW phases, except the trough, are
290 associated with significantly higher flash rates than the corresponding NDW phases valid at the
291 95% level. The trough value is similar for EADWs and NDWs over Africa. Consistent with
292 several previous studies which show a decrease in lightning over the ocean compared to land
293 (e.g., Christian et al. 2003), lightning decreases substantially over the East Atlantic compared to
294 Africa. Nevertheless, except in the southerly phase, all EADW flash rates over the East Atlantic
295 are greater than those of NDWs. But, these differences are relatively small (i.e., not significant
296 at the 99% level). Thus, the lightning data suggest that EADWs are generally associated with
297 more vigorous convection than that of NDWs.

298 Table 6 shows PCT_{37} and PCT_{85} values as a function of wave phase for various wave
299 types and regions. Differences between EADWs and NDWs over both Africa and the East
300 Atlantic are quite small and are not significant in any phase. Nevertheless, EADW values are
301 generally slightly less than those of NDWs over both regions, suggesting a slightly stronger ice
302 scattering signature and somewhat more vigorous convection for EADWs.

303 The difference between mean convective reflectivity values of EADWs and NDWs
304 (EADW minus NDW values) as a function of wave phase valid over the East Atlantic is shown
305 in Fig. 2. Note that differences are calculated and shown in Fig. 2 and all subsequent figures
306 only where the mean reflectivity values for both developing waves and NDWs are ≥ 18 dBZ (the

307 approximate minimum detectable signal of the PR; Yang et al. 2006). Differences are generally
308 positive in Fig. 2, indicating greater reflectivity values for EADWs. These larger reflectivity
309 values would presumably be associated with stronger updrafts and more vigorous convection in
310 order to support such reflectivity values. However, only the value at 2.5 km in the northerly
311 phase and 4.5–5.5 km in the southerly phase are significantly greater for EADWs (indicated by
312 squares in Fig. 2). Thus, considering how many levels and phases fail the significance tests, we
313 cannot infer much from the few levels that do show significance. In addition, the differences
314 between EADW and NDW reflectivity profiles over Africa (not shown) are also small and not
315 statistically significant.

316 In summary, EADWs appear to be associated with a greater *coverage* by convection and
317 cold cloudiness over both Africa and the East Atlantic compared to NDWs. There is only slight
318 indication of more intense convection associated with EADWs. These results are generally
319 consistent with the results of LP10 where developing waves were found to be associated with a
320 greater coverage by cold cloud tops and more lightning compared to NDWs. The coverage by
321 IR brightness temperatures ≤ 240 K and/or ≤ 210 K provide the greatest number of statistically
322 significant differences between EADWs and NDWs over both Africa and the East Atlantic, thus,
323 providing the best discrimination between EADWs and NDWs.

324 Some waves included in the NDW composite are associated with relatively little cold
325 cloudiness and convection and, from an operational forecasting perspective, would clearly be
326 distinguished from developing waves. Hence, a comparison between these NDWs and
327 developing waves is not particularly instructive. To make a comparison between developing
328 waves and NDWs associated with a similar probability of development, the archived Graphical
329 Tropical Weather Outlooks produced by the NHC were examined in order to identify easterly

330 waves that were assigned a moderate (30–50%) chance of genesis within 48 hours. Composites
331 were created for NDWs and all developing waves in 2009 and 2010 (the archived outlooks were
332 only available for the last two years of the study) at the times and locations when these waves
333 were assigned a 30–50% chance of genesis by the NHC. Forty-two (117) distinct easterly waves
334 (individual trough data points) were included in these developing wave composites. Note that 40
335 of these 42 waves actually developed within 48 hours. Nine (42) distinct waves (trough points)
336 were included in the NDW composites. Table 7 shows the statistics for these 30–50% chance-
337 of-genesis developing and NDW composites valid over the full analysis domain (to maximize
338 the sample size). Coverage by IR brightness temperatures ≤ 240 K, convective coverage, and
339 flash rates are greater in nearly all developing wave phases compared to the corresponding NDW
340 phases with the greatest differences generally found in the trough and northerly phases. In
341 addition, PCT_{37} values are smaller in all developing wave phases, except the southerly phase.
342 Therefore, when developing and NDWs were associated with an enhanced probability of
343 cyclogenesis according to the NHC, developing waves appear to be associated with more
344 widespread and intense convection, in general, in agreement with the results of the comparison
345 between all NDWs and EADWs. Note that none of the variables show statistically significant
346 differences between developing waves and NDWs associated with a moderate probability of
347 genesis, possibly due to relatively small sample sizes.

348 The climatological peak of tropical cyclone occurrence in the Atlantic occurs around
349 August–September (e.g., Landsea 1993). Hence, we wanted to examine possible intra-seasonal
350 impacts on our results by examining a comparison between EADWs and NDWs valid only for
351 August–September. In general, this comparison (not shown) revealed patterns similar to those
352 found for the comparison valid for June–November, especially over the East Atlantic (i.e.,

353 greater coverage and/or intensity of convection for EADWs). However, the magnitude of
354 differences between the two wave categories valid for the shortened time period were somewhat
355 smaller and less often statistically significant than observed for the comparison valid for the full
356 time period. Restricting the NDW composite to those waves that occur in August–September
357 may lead to a composite of waves that presumably propagate through an environment
358 climatologically more favorable for cyclogenesis (e.g., moister environment) and for more
359 widespread/intense convection compared to the full June–November sample.

360
361 *b. Comparison between West Atlantic – Caribbean Developing Waves and NDWs*
362

363
364 In order to increase the sample size (Table 2), waves that developed a tropical cyclone
365 over either the West Atlantic or Caribbean were combined into a single category (i.e., West
366 Atlantic – Caribbean developing waves; WACDWs). The coverage by certain IR thresholds
367 shown in Table 3 indicate that WACDWs are associated with significantly greater coverage by
368 cold cloud tops compared to NDWs in all phases except the ridge over Africa, the West Atlantic,
369 and the Caribbean. WACDW ridge values over these regions are also greater than those of
370 NDWs, but not with 99% level significance. Over the East Atlantic, only the coverage by cold
371 cloud tops in the trough phase is significantly greater for WACDWs. The coverage by cold
372 cloudiness in other WACDW phases over the East Atlantic is generally less than the
373 corresponding NDW values (the 240 K threshold in the southerly phase is actually significantly
374 less). Thus, a persistent large coverage by cold cloudiness in the trough phase may be important
375 for the genesis of tropical cyclones from WACDWs, while coverage by cold cloud tops in the
376 ridge phase is relatively unimportant for genesis.

377 The percentage convective coverage values shown for WACDWs and NDWs in Table 4
378 indicate few significant differences between the two wave categories over any longitude band.
379 In fact, only the WACDW trough over the West Atlantic is associated with significantly more
380 convective coverage than the NDW trough. The coverage in the WACDW northerly phase over
381 the Caribbean is also much greater than the corresponding NDW value, but the difference is only
382 significant at the 95% level. Despite the relative lack of statistically significant differences,
383 convective coverage is greater in all WACDW phases over Africa, the West Atlantic, and the
384 Caribbean (except for the ridge over Africa and trough over the Caribbean). Over the East
385 Atlantic, coverage in the WACDW trough and ridge is greater than the corresponding NDW
386 values, while northerly and southerly values are nearly identical between the two wave
387 categories over this band. Thus, convective coverage is generally larger for WACDWs over all
388 longitude bands, especially as these waves approach their genesis region over either the West
389 Atlantic or Caribbean.

390 None of the WACDW lightning flash rates are significantly different from those of
391 NDWs (Table 5) over any longitude band. However, over Africa and the Caribbean, flash rates
392 for all WACDW phases are greater than the corresponding NDW values. Flash rates over the
393 East and West Atlantic are also generally slightly greater for WACDWs. The mean PCTs from
394 deep convection in WACDWs (Table 6) also suggest no significant differences between
395 WACDW and NDW values with some values slightly greater for WACDWs and others slightly
396 greater for NDWs. Hence, the intensity of convection associated with WACDWs as indicated by
397 lightning and low PCTs does not appear to be all that different from that of NDWs.

398 The differences between mean vertical profiles of convective reflectivity for WACDWs
399 and NDWs as a function of wave phase over various longitude bands are shown in Fig. 3. Very

400 few of the differences between WACDWs and NDWs are significant. Only values at 3.5–4.5 km
401 in the northerly phase over the Caribbean and 3.5–5.5 km in the trough over the West Atlantic
402 are significantly greater for WACDWs. Despite the lack of significant differences, reflectivity
403 values are greater for WACDWs at all heights in all phases, except the ridge, as these waves
404 approach their genesis region over the Caribbean. In contrast, over Africa, NDWs are generally
405 associated with greater reflectivity values in all phases, except the northerly phase. Hence, as
406 WACDWs move from their origin over Africa to where they develop tropical cyclones over the
407 West Atlantic and Caribbean, convective reflectivity values associated with these waves
408 generally increase slightly relative to NDWs.

409 Similar to EADWs, the coverage by cold cloudiness (i.e., using IR thresholds) provides
410 the greatest number of statistically significant differences between WACDWs and NDWs and
411 appears to be the best discriminator between these two wave types, especially within the trough
412 phase. While convective coverage, lightning flash rates, mean cold PCTs, and convective
413 reflectivity provide few statistically significant differences between WACDWs and NDWs, these
414 variables appear to indicate that WACDWs are associated with a greater coverage and intensity
415 of convection as these waves approach their genesis region. This enhancement of convection
416 associated with WACDWs may help to moisten the larger-scale waves at mid/upper levels (e.g.,
417 Dunkerton et al. 2009) and/or increase larger-scale mid to low-level vorticity (e.g., Montgomery
418 et al. 2006; Nolan 2007; Raymond et al. 2011), helping to create an environment more favorable
419 for tropical cyclogenesis.

420 A comparison was also made between WACDWs and NDWs valid only for those months
421 when WACDWs are most active (i.e., August–October) as indicated by the annual distribution of

422 WACDW data points (not shown). Similar to EADWs, the restricted WACDW comparison
423 generally did not change the results obtained from the full June–November comparison.

424
425 *c. Comparison between East Pacific Developing Waves and NDWs*

426
427
428 Waves that developed tropical cyclones over the East Pacific (i.e., East Pacific
429 developing waves; EPDWs) are obviously a long distance from where they develop tropical
430 cyclones while the waves are near their origin over Africa, and there are several complicating
431 factors (e.g., topography of Central America; Zehnder 1991; Mozer and Zehnder 1996; Farfan
432 and Zehnder 1997; Zehnder et al. 1999; barotropic instability over the Caribbean and East
433 Pacific; Molinari et al. 1997) that could influence an EPDW between Africa and the East Pacific.
434 Hence, convection over Africa would not be expected to exert much of an influence on later
435 tropical cyclogenesis over the East Pacific. Nevertheless, EPDW lightning flash rates and
436 coverage by cold cloudiness valid for June–November (not shown) are significantly *greater* than
437 corresponding NDW values in various wave phases over Africa. However, the June–November
438 NDW composite over Africa includes all waves, including those waves that were too weak to
439 track all the way across the Atlantic and waves with relatively little convection. A comparison
440 between EPDW and NDW composites valid for only July and August (two of the most active
441 months for tropical cyclogenesis in the East Pacific), which restricts the NDW composite to
442 those waves that presumably move through an environment climatologically more favorable for
443 convection and for cyclogenesis, shows a much different pattern than that observed for June–
444 November. For example, the coverage by IR brightness temperatures below certain thresholds
445 over Africa valid for July–August only (Table 8) shows *smaller* EPDW coverage in all phases
446 (240 K threshold differences are significant in every phase, except the ridge phase, while 210 K

447 differences are significant in the trough and northerly phases) compared to the corresponding
448 NDW values. Thus, the focus of this subsection will be on a comparison between EPDWs and
449 NDWs valid for July–August because this restricted comparison appears to provide more
450 meaningful results than those obtained from the June–November comparison.

451 As EPDWs move over the East and West Atlantic, the coverage by cold cloudiness
452 (Table 8) becomes comparable to that of NDWs with some values greater for EPDWs and other
453 values greater for NDWs with no significant differences. Over the Caribbean and East Pacific,
454 all IR threshold coverage values are greater for EPDWs. Values are significantly greater in the
455 EPDW southerly phase over the Caribbean and all phases over the East Pacific (except for the
456 210 K value in the ridge). Convective coverage (not shown) is generally greater for NDWs over
457 Africa, the East Atlantic, and West Atlantic, but differences between these waves and EPDWs
458 are generally not significant. In contrast, convective coverage is often greater for EPDWs over
459 the Caribbean and East Pacific with significantly greater values in the southerly phase over the
460 Caribbean and northerly and southerly phases over the East Pacific. Thus, relative to NDWs,
461 convective and cold cloudiness coverage is smaller for EPDWs over Africa and generally
462 increases as EPDWs move across the Atlantic and approach their genesis region.

463 Composite lightning flash rates for EPDWs and NDWs (Table 9) indicate that flash rates
464 are smaller in all EPDW phases over Africa compared to the corresponding NDW values, but
465 differences are not significant. Over the East Atlantic, West Atlantic, and Caribbean, flash rates
466 are comparable between EPDWs and NDWs with some values greater for EPDWs and others
467 greater for NDWs. When EPDWs are over the East Pacific where they develop tropical
468 cyclones, flash rates in all phases of these waves are greater (significantly greater in all but the
469 ridge phase) than the corresponding NDW values.

470 A comparison between EPDW and NDW cold PCTs (not shown) indicates, similar to
471 other developing waves, little difference between the two wave types. However, over the East
472 Pacific, EPDW trough and southerly phase PCT_{85} values are significantly less than the
473 corresponding NDW values, suggesting more intense convection for these waves near their
474 genesis region. Overall, though, differences between developing waves (EADWs, WACDWs,
475 and EPDWs) and NDWs in terms of mean cold PCTs are quite small over all longitude bands,
476 suggesting that this way of comparing PCTs (taking the mean of pixels below a threshold for
477 deep convection) may not be the best use of passive microwave information.

478 Over all longitude bands east of the East Pacific band, differences between EPDWs and
479 NDWs in terms of mean convective reflectivity profiles (not shown) are generally small with few
480 statistically significant differences. Differences in convective reflectivity profiles between
481 EPDWs and NDWs over the East Pacific (Fig. 4) indicate generally greater values for EPDWs in
482 all phases at all levels. EPDW values are significantly greater between 2.5 and 5.5 km in the
483 northerly phase, at 2.5 km in the trough, and at 3.5 km in the southerly phase. Thus, when
484 EPDWs are near their origin over Africa, differences between these waves and NDWs in terms
485 of convective reflectivity are small. Differences remain small until EPDWs move over their
486 genesis region of the East Pacific, where low- to mid-level reflectivity values become
487 significantly greater for these waves in all phases other than the ridge.

488 In summary, EPDW convective coverage and/or intensity appear to be relatively low
489 compared to NDWs near their origin over Africa. As EPDWs move across the Atlantic,
490 Caribbean, and into the East Pacific region, convective coverage and/or intensity gradually
491 become significantly greater than that of NDWs. The pronounced increase in convection over
492 the Caribbean and East Pacific may be related to barotropic instability found over these regions

493 (Molinari et al. 1997). It is possible that this instability over the Caribbean and East Pacific
494 could help amplify easterly waves, perhaps helping to spawn more convection within the waves
495 over these regions. In addition, the Caribbean region may be associated with an enhancement of
496 convection due to the large landmasses in that region (cf. Fig. 1). Note that both EPDWs and
497 NDWs are subject to the effects of land and its associated diurnal cycle of convection over the
498 Caribbean region. Thus, any differences observed between these two wave types in terms of
499 characteristics of convection should not be due to land/ocean differences.

500 In contrast to EADWs and WACDWs where the coverage by IR thresholds was clearly
501 the one variable that could provide the best discrimination between these waves and NDWs,
502 several variables could potentially be used to separate EPDWs from NDWs over the East Pacific,
503 including IR thresholds, lightning flash rates, and low-level PR convective reflectivity values.
504 This may suggest that the coverage and intensity of convection over the East Pacific are
505 important for tropical cyclogenesis over this region.

506 Based on NHC (2011), some waves spawned a tropical cyclone in both the Atlantic and
507 East Pacific basins. To determine if there were any differences in terms of convective
508 characteristics between these waves which spawned multiple cyclones and those which spawned
509 only one storm, composites were created for waves that developed multiple cyclones. However,
510 few significant differences were found between multiple and single cyclone waves. Waves
511 which develop multiple cyclones may lend themselves better to case study analysis which is left
512 for future work.

513 Again using information from NHC (2011), developing waves were also separated
514 according to whether the subsequent tropical cyclone achieved hurricane strength or only tropical
515 storm strength. Composites were also created for both of these wave categories. Except for

516 some differences between hurricane and tropical storm waves over the West Atlantic, the
517 convective characteristics of hurricane and tropical storm waves are generally not significantly
518 different. These results are not surprising because many other factors (e.g., SSTs, wind shear)
519 help control the final strength of a tropical cyclone. In addition, because we are not controlling
520 for large-scale conditions, the relative enhancement of convection in hurricane waves over the
521 West Atlantic could be a result of large-scale conditions favorable for both convection and
522 intensification to hurricane strength. In this case, the enhanced convection in the precursor wave
523 is not a factor responsible for intensification to hurricane strength.

524 525 **4. Summary and Conclusions**

526
527
528 This study examines the characteristics of convection and cold cloudiness associated with
529 tropical easterly waves using data from the Tropical Rainfall Measurement Mission (TRMM)
530 Lightning Imaging Sensor, Precipitation Radar (PR), and Microwave Imager as well as IR
531 brightness temperatures from the NASA global-merged dataset. In particular, the purpose of the
532 study was to determine which characteristics or observations of convection provide the best
533 distinction between developing waves and nondeveloping waves (NDWs) and over which
534 regions. Another goal of the study was to determine whether the convective characteristics that
535 provide the best distinction between the two wave types vary for waves that develop tropical
536 cyclones over different regions.

537 Results suggest that the variables that provide the best distinction between developing
538 waves and NDWs do vary between the Atlantic and East Pacific. In particular, the coverage by
539 IR brightness temperatures ≤ 240 K and ≤ 210 K appear to provide the largest distinction between
540 East Atlantic developing waves (EADWs; waves which developed a tropical cyclone over the

541 East Atlantic) and NDWs in all wave phases over Africa and in the trough and northerly phases
542 over the East Atlantic. The coverage by IR thresholds also provides the best distinction between
543 West Atlantic – Caribbean developing waves (WACDWs; waves which spawned a cyclone over
544 either the West Atlantic or Caribbean) and NDWs. In particular, the coverage by cold cloudiness
545 was found to be significantly greater for WACDWs in all phases, except the ridge, over all
546 longitude bands but the East Atlantic (values are only significantly greater for WACDWs in the
547 trough over the East Atlantic). Thus, results for WACDWs indicate that a persistent large
548 coverage by cold cloudiness in the trough phase may be important for cyclogenesis from these
549 waves. The fact that indices of the coverage by convection/cold cloudiness provide a better
550 discrimination between developing waves over the Atlantic and NDWs than indicators of
551 convective intensity (e.g., lightning flash rates, polarization corrected temperatures) suggests that
552 the coverage by convection is more important than intensity for tropical cyclogenesis over the
553 Atlantic.

554 In contrast to waves which developed a tropical cyclone over the Atlantic basin, waves
555 which spawned a tropical cyclone over the East Pacific (East Pacific developing waves; EPDWs)
556 are associated with statistically significantly greater IR threshold coverage, convective coverage,
557 lightning flash rates, and low-level PR convective reflectivity in various wave phases (no clear
558 preference for enhanced convection in any one wave phase over another) when compared to
559 NDWs over the East Pacific. In contrast to what was found for EADWs and WACDWs,
560 restricting the comparison between EPDWs and NDWs to only the most active months for East
561 Pacific cyclogenesis led to quite different results from the corresponding comparison valid for
562 June–November, especially over Africa. This suggests that care must be taken in selecting a

563 temporal domain for a comparison between EPDWs and NDWs and/or selecting a sample of
564 NDWs.

565 Future work could involve developing thresholds based on the most relevant convective
566 parameters to help provide an indication of enhanced probability (or lack thereof) of tropical
567 cyclogenesis. For example, Table 10 lists the most relevant parameters for EADWs, WACDWs,
568 and EPDWs over various regions and initial thresholds that could be tested for each parameter.
569 These thresholds are based approximately on the 99% significance level for the sample sizes
570 used for this study. Other future work could involve incorporating these convective indicators
571 that provide the greatest distinction between developing waves and NDWs in the development of
572 a statistical cyclogenesis/hurricane prediction model.

573
574 *Acknowledgements.*

575
576
577 This work was part of the lead author's research for his doctoral degree, and funding for the
578 research was provided through a NASA Earth and Space Science Fellowship, Grant
579 #NNX09AO40H. Dr. Walter Petersen and Dr. Daniel Cecil also acknowledge funding from the
580 NASA PMM/TRMM Program. Suggestions from Dr. Ron McTaggart-Cowan and two
581 anonymous reviewers greatly improved an earlier version of this manuscript. The authors would
582 also like to gratefully acknowledge the Goddard Earth Sciences Data and Information Services
583 Center for providing the TMI, PR, and IR brightness temperature data, the NASA EOSDIS
584 Global Hydrology Resource Center DAAC for providing the LIS science data, and the
585 NOAA/OAR/ESRL PSD for providing the NCEP-NCAR reanalysis data.

586

587

588
589
590
591
592
593
594
595
596
597
598
599
600
601
602
603
604
605
606
607
608
609

REFERENCES

Avila, L. A., 1991: Eastern North Pacific hurricane season of 1990. *Mon. Wea. Rev.*, **119**, 2034–2046.

_____, and R. J. Pasch, 1992: Atlantic tropical systems of 1991. *Mon. Wea. Rev.*, **120**, 2688–2696.

Awaka, J., T. Iguchi, and K. Okamoto, 1998: Early results on rain type classification by the Tropical Rainfall Measuring Mission (TRMM) precipitation radar. *Proc. Eighth URSI Commission F. Triennial Open Symp.*, Aveiro, Portugal, International Union of Radio Science, 143–146.

_____, _____, and _____, 2009, TRMM PR standard algorithm 2A23 and its performance on bright band detection. *J. Meteor. Soc. Japan*, **87A**, 31–52.

Berry, G. J., and C. Thorncroft, 2005: Case study of an intense African easterly wave. *Mon. Wea. Rev.*, **133**, 752–766.

Boccippio, D. J., S. J. Goodman, and S. Heckman, 2000: Regional differences in tropical lightning distributions. *J. Appl. Meteor.*, **39**, 2231–2248.

_____, W. J. Koshak, and R. J. Blakeslee, 2002: Performance assessment of the optical transient detector and lightning imaging sensor. Part I: Predicted diurnal variability. *J. Atmos. Oceanic Technol.*, **19**, 1318–1332.

Bracken, W. E., and L. F. Bosart, 2000: The role of synoptic-scale flow during tropical cyclogenesis over the North Atlantic Ocean. *Mon. Wea. Rev.*, **128**, 353–376.

Burpee, R. W., 1972: The origin and structure of easterly waves in the lower troposphere of North Africa. *J. Atmos. Sci.*, **29**, 77–89.

610 _____, 1974: Characteristics of North African easterly waves during the summers of 1968 and
611 1969. *J. Atmos. Sci.*, **31**, 1556–1570.

612 Carlson, T. N., 1969: Synoptic histories of three African disturbances that developed into
613 Atlantic hurricanes. *Mon. Wea. Rev.*, **97**, 256–276.

614 Cecil, D. J., and E. J. Zipser, 1999: Relationships between tropical cyclone intensity and
615 satellite-based indicators of inner core convection: 85-GHz ice-scattering signature and
616 lightning. *Mon. Wea. Rev.*, **127**, 103–123.

617 _____, _____, and S. W. Nesbitt, 2002: Reflectivity, ice scattering, and lightning
618 characteristics of hurricane eyewalls and rainbands. Part I: Quantitative description. *Mon.*
619 *Wea. Rev.*, **130**, 769–784.

620 _____, and _____, 2002: Reflectivity, ice scattering, and lightning characteristics of hurricane
621 eyewalls and rainbands. Part II: Intercomparison of observations. *Mon. Wea. Rev.*, **130**,
622 785–801.

623 Christian, H. J., R. J. Blakeslee, and S. L. Goodman, 1992: Lightning Imaging Sensor (LIS) for
624 the Earth Observing System. NASA TM-4350, 36 pp.

625 _____, 1999: *Atmospheric Electricity*, Guntersville, AL, NASA/CP-1999-209261, 715–718.

626 _____, and Coauthors, 2003: Global frequency and distribution of lightning as observed from
627 space by the optical transient detector. *J. Geophys. Res.*, **108**, 4005,
628 doi:10.1029/2002JD002347.

629 Chronis, T. G., E. R. Williams, E. N. Anagnostou, and W. A. Petersen, 2007: African lightning:
630 Indicator of tropical Atlantic cyclone formation. *Eos, Trans. Amer. Geophys. Union*, **88**,
631 397–398.

632 Deierling, W., and W. A. Petersen, 2008: Total lightning activity as an indicator of updraft
633 characteristics. *J. Geophys. Res.*, **113**, D16210, doi:10.1029/2007JD009598.

634 Dunkerton, T. J., M. T. Montgomery, and Z. Wang, 2009: Tropical cyclogenesis in a tropical
635 wave critical layer: Easterly waves. *Atmos. Chem. Phys.*, **9**, 5587–5646.

636 Duvel, J-Ph., 1990: Convection over tropical Africa and the Atlantic Ocean during northern
637 summer. Part II: Modulation by easterly waves. *Mon. Wea. Rev.*, **118**, 1855–1868.

638 Farfan, L. M., and J. A. Zehnder, 1997: Orographic influence on the synoptic-scale circulations
639 associated with the genesis of Hurricane Guillermo (1991). *Mon. Wea. Rev.*, **125**,
640 2683–2698.

641 Gray, W. M., 1968: Global view of the origin of tropical disturbances and storms. *Mon. Wea.*
642 *Rev.*, **96**, 669–700.

643 Gu, G., R. F. Adler, G. J. Huffman, and S. Curtis, 2004: African easterly waves and their
644 association with precipitation. *J. Geophys. Res.*, **109**, D04101,
645 doi:10.1029/2003/JD003967.

646 Hendricks, E. A., M. T. Montgomery, and C. A. Davis, 2004: The role of “vortical” hot towers in
647 the formation of tropical cyclone Diana (1984). *J. Atmos. Sci.*, **61**, 1209–1232.

648 Hopsch, S. B., C. D. Thorncroft, and K. R. Tyle, 2010: Analysis of African easterly wave
649 structures and their role in influencing tropical cyclogenesis. *Mon. Wea. Rev.*, **138**, 1399–
650 1419.

651 Houze, R. A., Jr., W.-C. Lee, and M. M. Bell, 2009: Convective contribution to the genesis of
652 Hurricane Ophelia (2005). *Mon. Wea. Rev.*, **137**, 2778–2800.

653 Iguchi, T., T. Kozu, R. Meneghini, J. Awaka, and K. Okamoto, 2000: Rain-profiling
654 algorithm for the TRMM precipitation radar. *J. Appl. Meteor.*, **39**, 2038–2052.

655 _____, _____, J. Kwiatkowski, R. Meneghini, J. Awaka, and K. Okamoto, 2009:
656 Uncertainties in the rain profiling algorithm for the TRMM precipitation radar. *J. Meteor.*
657 *Soc. Japan*, **87A**, 1–30.

658 Kalnay, E., and Coauthors, 1996: The NCEP/NCAR 40-year reanalysis project. *Bull. Amer.*
659 *Meteor. Soc.*, **77**, 437–471.

660 Kozu, T., and Coauthors, 2001: Development of precipitation radar onboard the Tropical
661 Rainfall Measuring Mission (TRMM) satellite. *IEEE Trans. Geosci. Remote Sens.*, **39**,
662 102–116.

663 Kummerow, C., W. Barnes, T. Kozu, J. Shiue, and J. Simpson, 1998: The tropical rainfall
664 measuring mission (TRMM) sensor package. *J. Atmos. Oceanic Technol.*, **15**, 809–817.

665 Kurihara, Y., and R. E. Tuleya, 1981: A numerical simulation study on the genesis of a tropical
666 storm. *Mon. Wea. Rev.*, **109**, 1629–1653.

667 Landsea, C. W., 1993: A climatology of intense (or major) Atlantic hurricanes. *Mon. Wea. Rev.*,
668 **121**, 1703–1713.

669 _____, G. D. Bell, W. M. Gray, and S. B. Goldenberg, 1998: The extremely active 1995
670 Atlantic hurricane season: Environmental conditions and verification of seasonal
671 forecasts. *Mon. Wea. Rev.*, **126**, 1174–1193.

672 Leary, L. A., and E. A. Ritchie, 2009: Lightning flash rates as an indicator of tropical
673 cyclone genesis in the Eastern North Pacific. *Mon. Wea. Rev.*, **137**, 3456–3470.

674 Leppert, K. D., II, and W. A. Petersen, 2010: Electrically-active hot towers in African
675 easterly waves prior to tropical cyclogenesis. *Mon. Wea. Rev.*, **138**, 663–687.

676 _____, and D. J. Cecil, 2012: African easterly wave convection and tropical cyclogenesis: A
677 Lagrangian perspective. *Extended Abstracts, 30th Conf. on Hurricanes and Tropical*
678 *Meteorology*, Ponte Vedra Beach, FL, Amer. Meteor. Soc., 3C.6.

679 Liu, Z., D. Ostrenga, G. G. Leptoukh, and A. V. Mehta, 2009: Online visualization and analysis
680 of global half-hourly pixel-resolution infrared dataset. *Extended Abstracts, 25th Conf. on*
681 *International Interactive Information and Processing Systems (IIPS) for Meteorology,*
682 *Oceanography, and Hydrology*, Phoenix, AZ, Amer. Meteor. Soc., J3.4.

683 Meneghini, R., T. Iguchi, T. Kozu, L. Liao, K. Okamoto, J. A. Jones, and J. Kwiatkowski, 2000:
684 Use of the surface reference technique for path attenuation estimates from the TRMM
685 precipitation radar. *J. Appl. Meteor.*, **39**, 2053–2070.

686 Mohr, K. I., and E. J. Zipser, 1996: Defining mesoscale convective systems by their 85-GHz ice-
687 scattering signatures. *Bull. Amer. Meteor. Soc.*, **77**, 1179–1189.

688 _____, J. S. Famiglietti, and E. J. Zipser, 1999: The contribution to tropical rainfall with
689 respect to convective system type, size, and intensity estimated from the 85-GHz ice-
690 scattering signature. *J. Appl. Meteor.*, **38**, 596–606.

691 Molinari, J., and D. Vollaro, 2000: Planetary- and synoptic-scale influences on Eastern Pacific
692 tropical cyclogenesis. *Mon. Wea. Rev.*, **128**, 3296–3307.

693 _____, D. Knight, M. Dickinson, D. Vollaro, and S. Skubis, 1997: Potential vorticity, easterly
694 waves, and Eastern Pacific tropical cyclogenesis. *Mon. Wea. Rev.*, **125**, 2699–2708.

695 Montgomery, M. T., M. E. Nicholls, T. A. Cram, and A. B. Saunders, 2006: A vortical hot tower
696 route to tropical cyclogenesis. *J. Atmos. Sci.*, **63**, 355–386.

697 Mozer, J. B., and J. A. Zehnder, 1996: Lee vorticity production by large-scale tropical mountain
698 ranges. Part I: Eastern North Pacific tropical cyclogenesis. *J. Atmos. Sci.*, **53**, 521–538.

699 National Hurricane Center, cited 2011: NHC archive of hurricane seasons. [Available online at
700 <http://www.nhc.noaa.gov/pastall.shtml>.]

701 Nolan, D. S., 2007: What is the trigger for tropical cyclogenesis? *Aust. Meteorol. Mag.*, **56**, 241–
702 266.

703 Norquist, D. C., E. E. Recker, and R. J. Reed, 1977: The energetics of wave disturbances as
704 observed during phase III of GATE. *Mon. Wea. Rev.*, **105**, 334–342.

705 Panofsky, H. A., and G. W. Brier, 1958: *Some applications of statistics to meteorology*. The
706 Pennsylvania State University, 224 pp.

707 Petersen, W. A., R. Cifelli, D. J. Boccippio, S. A. Rutledge, and C. Fairall, 2003: Convection and
708 easterly wave structures observed in the eastern Pacific warm pool during EPIC-2001. *J.*
709 *Atmos. Sci.*, **60**, 1754–1773.

710 _____, and D. J. Boccippio, 2004: Variability of convective structure and lightning activity in
711 tropical easterly waves. Preprints, *26th Conf. on Hurricanes and Tropical Meteorology*,
712 Miami Beach, FL, Amer. Meteor. Soc.

713 Price, C., Y. Yair, and M. Asfur, 2007: East African lightning as a precursor of Atlantic
714 hurricane activity. *Geophys. Res. Lett.*, **34**, L09805, doi:10.1029/2006GL028884.

715 Raymond, D. J., S. L. Sessions, and C. Lopez Carrillo, 2011: Thermodynamics of tropical
716 cyclogenesis in the northwest Pacific. *J. Geophys. Res.*, **116**, D18101,
717 doi:10.1029/2011JD015624.

718 Reasor, P. D., M. T. Montgomery, and L. F. Bosart, 2005: Mesoscale observations of the genesis
719 of Hurricane Dolly (1996). *J. Atmos. Sci.*, **62**, 3151–3171.

720 Reed, R. J., D. C. Norquist, and E. E. Recker, 1977: The structure and properties of African
721 wave disturbances as observed during phase III of GATE. *Mon. Wea. Rev.*, **105**, 317–
722 333.

723 Ritchie, E. A., and G. J. Holland, 1997: Scale interactions during the formation of Typhoon
724 Irving. *Mon. Wea. Rev.*, **125**, 1377–1396.

725 Rotunno, R., and K. A. Emanuel, 1987: An air–sea interaction theory for tropical cyclones. Part
726 II: Evolutionary study using a non-hydrostatic axisymmetric numerical model. *J. Atmos.*
727 *Sci.*, **44**, 542–561.

728 Rutledge, S. A., E. R. Williams, and T. D. Keenan, 1992: The down under Doppler and
729 electricity experiment (DUNDEE): Overview and preliminary results. *Bull. Amer.*
730 *Meteor. Soc.*, **73**, 3–16.

731 Saunders, C. P. R., and S. L. Peck, 1998: Laboratory studies of the influence of the rime
732 accretion rate on charge transfer during crystal/graupel collisions. *J. Geophys. Res.*, **103**,
733 13949–13956.

734 Serra, Y. L., G. N. Kiladis, and M. F. Cronin, 2008: Horizontal and vertical structure of
735 easterly waves in the Pacific ITCZ. *J. Atmos. Sci.*, **65**, 1266–1284.

736 _____, _____, and K. I. Hodges, 2010: Tracking and mean structure of easterly waves over
737 the Intra-Americas Sea. *J. Climate*, **23**, 4823–4840.

738 Sippel, J. A., J. W. Nielsen-Gammon, and S. E. Allen, 2006: The multiple-vortex nature of
739 tropical cyclogenesis. *Mon. Wea. Rev.*, **134**, 1796–1814.

740 Smith, E. A., H. J. Cooper, X. Xiang, A. Mugnai, and G. J. Tripoli, 1992: Foundations for
741 statistical-physical precipitation retrieval from passive microwave satellite measurements.

742 Part I: Brightness temperature properties of a time-dependent cloud-radiation model. *J.*
743 *Appl. Meteor.*, **31**, 506–531.

744 Spencer, R. W., H. M. Goodman, and R. E. Hood, 1989: Precipitation retrieval over land and
745 ocean with the SSM/I: Identification and characteristics of the scattering signal. *J. Atmos.*
746 *Oceanic Technol.*, **6**, 254–273.

747 Takahashi, T., 1978: Riming electrification as a charge generation mechanism in thunderstorms.
748 *J. Atmos. Sci.*, **35**, 1536–1548.

749 Thompson, R. M., S. W. Payne, E. E. Recker, and R. J. Reed, 1979: Structure and properties of
750 synoptic-scale wave disturbances in the intertropical convergence zone of the eastern
751 Atlantic. *J. Atmos. Sci.*, **36**, 53–72.

752 Thorncroft, C. D., N. M. J. Hall, and G. N. Kiladis, 2008: Three-dimensional structure and
753 dynamics of African easterly waves. Part III: Genesis. *J. Atmos. Sci.*, **65**, 3596–3607.

754 Toracinta, E. R., D. J. Cecil, E. J. Zipser, and S. W. Nesbitt, 2002: Radar, passive microwave,
755 and lightning characteristics of precipitating systems in the tropics. *Mon. Wea. Rev.*, **130**,
756 802–824.

757 Williams, E. R., S. A. Rutledge, S. G. Geotis, N. Renno, E. Rasmussen, and T. Rickenbach,
758 1992: A radar and electrical study of tropical “hot towers.” *J. Atmos. Sci.*, **49**, 1386–1395.

759 Yang, S., W. S. Olson, J.-J. Wang, T. L. Bell, E. A. Smith, and C. D. Kummerow, 2006:
760 Precipitation and latent heating distributions from satellite passive microwave
761 radiometry. Part II: Evaluation of estimates using independent data. *J. Appl. Meteor.*
762 *Climatol.*, **45**, 721–739.

763 Zehnder, J. A., 1991: The interaction of planetary-scale tropical easterly waves with topography:
764 A mechanism for the initiation of tropical cyclones. *J. Atmos. Sci.*, **448**, 1217–1230.

765 _____, D. M. Powell, and D. L. Ropp, 1999: The interaction of easterly waves, orography, and
766 the intertropical convergence zone in the genesis of eastern Pacific tropical cyclones.

767 *Mon. Wea. Rev.*, **127**, 1566–1585.

768 Zipser, E. J., 1994: Deep cumulonimbus cloud systems in the tropics with and without lightning.

769 *Mon. Wea. Rev.*, **122**, 1837–1851.

770

771

772

773

774

775

776

777

778

779

780

781

782

783

784

785

786

787

788 **List of Figures**

789

790

791

792 1 Map showing the location of the full analysis domain (130°W–20°E) and smaller

793 longitude bands utilized for this study. EPC represents the East Pacific band, CAR the

794 Caribbean and Central America band, WAT the West Atlantic band, EAT the East

795 Atlantic band, and AFR the Africa longitude band 37

796 2 Precipitation Radar (PR) convective reflectivity (only values classified as convective are

797 used) differences between East Atlantic developing waves (EADWs) and nondeveloping

798 waves (NDWs; i.e., EADW minus NDW values) as a function of height and wave phase

799 *valid over the East Atlantic*. The dashed horizontal lines depict the value of the standard

800 deviation at each height, and the squares indicate EADW values that are significantly

801 greater than the corresponding values of NDWs valid at the 99% level 38

802 3 Precipitation Radar convective reflectivity (only values classified as convective are used)

803 differences between West Atlantic – Caribbean developing waves (WACDWs) and

804 nondeveloping waves (NDWs; i.e., WACDW minus NDW values) as a function of height

805 and wave phase *valid over a.) Africa b.) the East Atlantic c.) the West Atlantic, and d.) the*

806 *Caribbean*. The dashed horizontal lines depict the value of half the standard deviation at

807 each height, and the squares indicate WACDW values that are significantly greater than

808 the corresponding NDW values valid at the 99% level 39

809 4 Precipitation Radar (PR) convective reflectivity (only values classified as convective are

810 used) differences between East Pacific developing waves (EPDWs) and nondeveloping

811 waves (NDWs; i.e., EPDW minus NDW values) as a function of height and wave phase

812 *valid over the East Pacific* valid for July–August only. The dashed horizontal lines

813 depict the value of half the standard deviation at each height, and the squares indicate
814 EPDW values that are significantly greater than the corresponding NDW values valid at
815 the 99% level..... 41

816

817

818

819

820

821

822

823

824

825

826

827

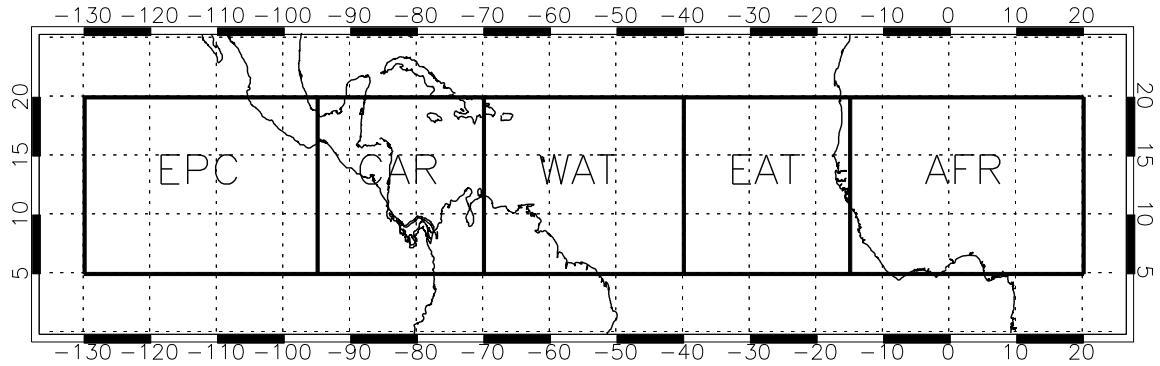
828

829

830

831

832

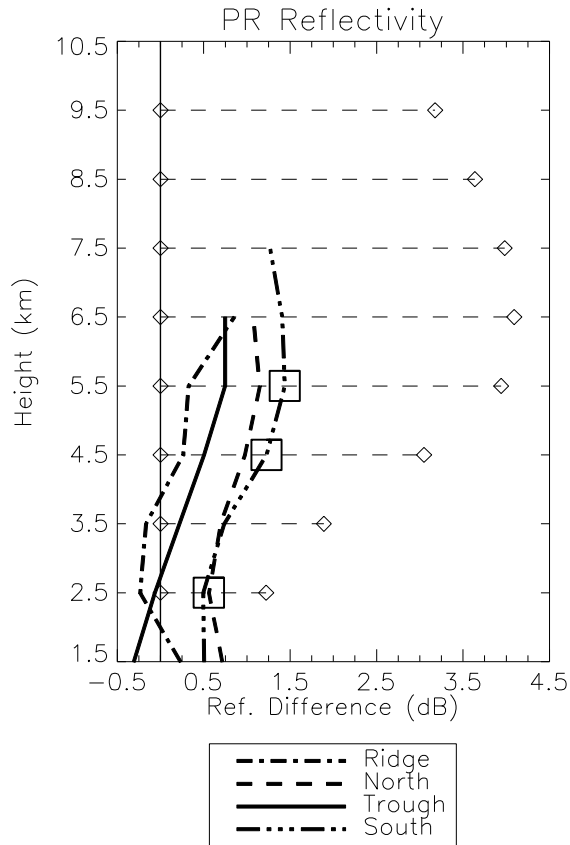


833

834 FIG. 1. Map showing the location of the full analysis domain (130°W–20°E) and smaller
 835 longitude bands utilized for this study. EPC represents the East Pacific band, CAR the
 836 Caribbean and Central America band, WAT the West Atlantic band, EAT the East Atlantic band,
 837 and AFR the Africa longitude band.

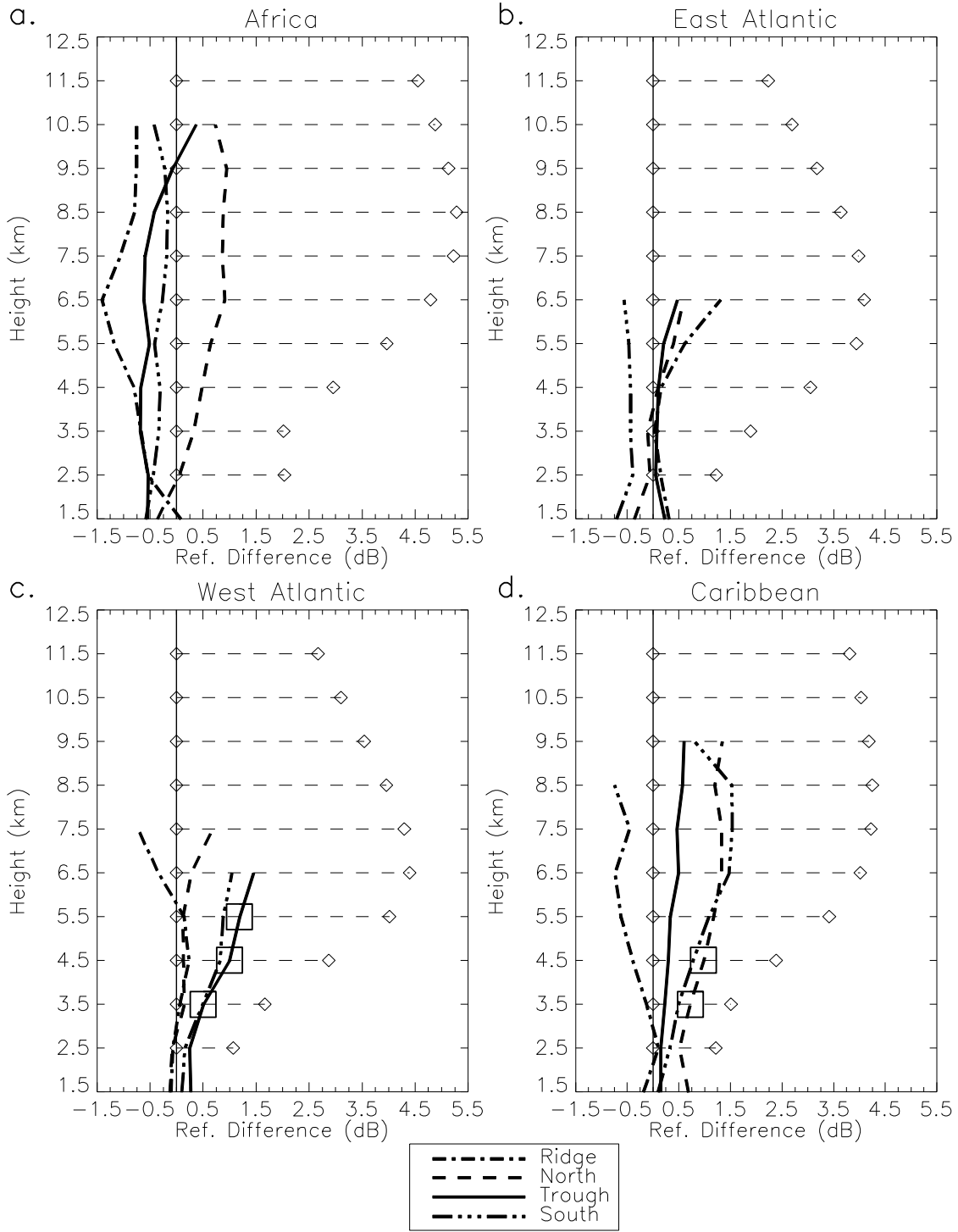
838

839



840

841 FIG. 2. Precipitation Radar (PR) convective reflectivity (only values classified as convective are
 842 used) differences between East Atlantic developing waves (EADWs) and nondeveloping waves
 843 (NDWs; i.e., EADW minus NDW values) as a function of height and wave phase *valid over the*
 844 *East Atlantic*. The dashed horizontal lines depict the value of half the standard deviation at each
 845 height, and the squares indicate EADW values that are significantly greater than the
 846 corresponding values of NDWs valid at the 99% level.



847

848 FIG. 3. Precipitation Radar convective reflectivity (only values classified as convective are used)

849 differences between West Atlantic – Caribbean developing waves (WACDWs) and

850 nondeveloping waves (NDWs; i.e., WACDW minus NDW values) as a function of height and
851 wave phase *valid over* a.) *Africa* b.) *the East Atlantic* c.) *the West Atlantic*, and d.) *the*
852 *Caribbean*. The dashed horizontal lines depict the value of half the standard deviation at each
853 height, and the squares indicate WACDW values that are significantly greater than the
854 corresponding NDW values valid at the 99% level.

855

856

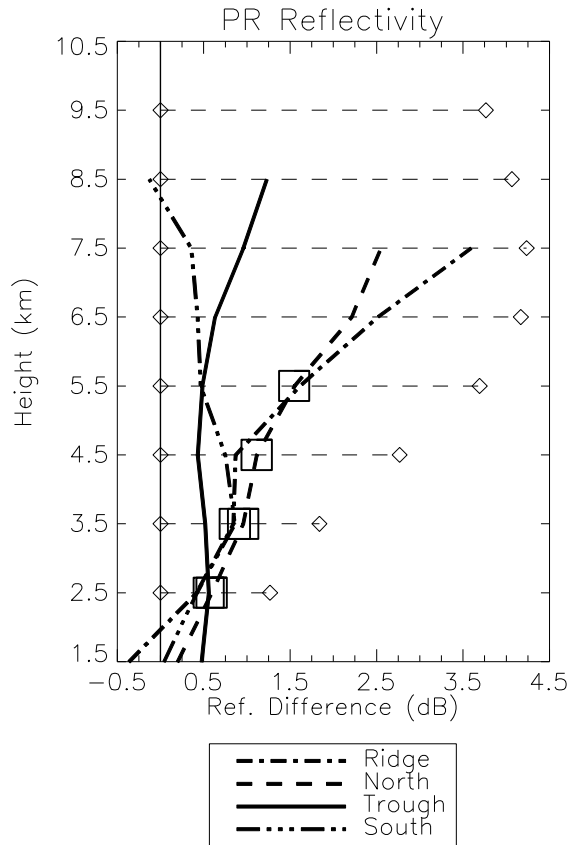
857

858

859

860

861



862

863 FIG. 4. Precipitation Radar (PR) convective reflectivity (only values classified as convective are
 864 used) differences between East Pacific developing waves (EPDWs) and nondeveloping waves
 865 (NDWs; i.e., EPDW minus NDW values) as a function of height and wave phase *valid over the*
 866 *East Pacific* valid for July–August only. The dashed horizontal lines depict the value of half the
 867 standard deviation at each height, and the squares indicate EPDW values that are significantly
 868 greater than the corresponding NDW values valid at the 99% level.

869

870

871

872

873

874

875

876 **List of Tables**

877

878

879

880 1 Definitions and acronyms associated with various wave categories used in this study ... 45

881 2 The number of distinct easterly waves and data points used for the trough composites of

882 nondeveloping waves (NDWs), East Atlantic developing waves (EADWs), West Atlantic

883 – Caribbean developing waves (WACDWs), and East Pacific developing waves

884 (EPDWs). The numbers of distinct waves are valid over the full analysis domain (ALL)

885 while the trough points are valid over individual longitude bands (bands defined as in

886 Fig. 1). The asterisk indicates wave categories that are valid for July–August only. The

887 number of individual NDWs is an estimate and includes an estimate of uncertainty

888 because of the difficulty in counting these waves (see text). Finally, the missing values

889 are for those composites that were unavailable 46

890 3 The fractional coverage by IR brightness temperatures ≤ 240 K and ≤ 210 K for East

891 Atlantic developing wave (EADW), West Atlantic – Caribbean developing wave

892 (WACDW), and nondeveloping wave (NDW) phases valid over various longitude bands.

893 The bold (italic) numbers indicate values that are significantly greater (less) than the

894 corresponding NDW values valid at the 99% level 47

895 4 Percentage convective coverage as a function of wave phase for East Atlantic developing

896 waves (EADWs), West Atlantic – Caribbean developing waves (WACDWs), and

897 nondeveloping waves (NDWs) valid over various longitude bands. The bold and italic

898 values are as in Table 3 48

899 5 As in Table 4, except for lightning flash rates (flashes day⁻¹) 49

900 6 Mean polarization corrected temperatures at 37.0 and 85.5 GHz using 37.0-GHz values
901 ≤ 260 K and 85.5-GHz values ≤ 200 K (i.e., values associated with deep convection) for
902 East Atlantic developing wave (EADW), West Atlantic – Caribbean developing wave
903 (WACDW), and nondeveloping wave (NDW) phases valid over various longitude bands.
904 No EADW or WACDW values are significantly different from those of NDWs valid at
905 the 99% level..... 50

906 7 The fractional coverage by IR brightness temperatures ≤ 240 K and ≤ 210 K, mean
907 polarization corrected temperatures (K) at 37.0 and 85.5 GHz using the same thresholds
908 as in Table 6, convective coverage (%), and lightning flash rates (flashes day⁻¹) for
909 developing and nondeveloping waves (30–50% Dev. and 30–50% ND, respectively) that
910 were assigned a 30–50% probability of development within the next 48 hours by the
911 National Hurricane Center. Note that none of the 30–50% Dev. values are significantly
912 different from the corresponding 30–50% ND values valid at the 99% level..... 51

913 8 The fractional coverage by IR brightness temperatures ≤ 240 K and ≤ 210 K for East
914 Pacific developing wave (EPDW) and nondeveloping wave (NDW) phases valid over
915 various longitude bands using only data valid for July and August. The bold and italic
916 values are as in Table 3..... 52

917 9 Lightning flash rates (flashes day⁻¹) for East Pacific developing wave (EPDW) and
918 nondeveloping wave (NDW) phases valid over various longitude bands using only data
919 valid for July and August. The bold and italic values are as in Table 3..... 53

920 10 A summary of the convective parameters that provide the greatest distinction between
921 nondeveloping waves and East Atlantic developing waves (EADWs), West Atlantic –
922 Caribbean developing waves (WACDWs), and East Pacific developing waves (EPDWs)

923 over various regions (EAT = East Atlantic, WAT = West Atlantic, CAR = Caribbean, and
924 EPC = East Pacific) in various phases. Suggested thresholds to initially be tested to
925 determine the utility of these parameters for tropical cyclogenesis forecasting are also
926 provided. Note that the 240 K and 210 K IR coverage thresholds are nondimensional,
927 while the flash rate threshold has units of flashes day⁻¹ 54

928

929

930

931

932

933

934

935

936

937

938

939

940

941

942

943

944

945

946

947 TABLE 1. Definitions and acronyms associated with various wave categories used in this study.

Wave Category	Acronym	Definition
East Atlantic developing wave	EADW	Wave developed a tropical depression over the East Atlantic longitude band
West Atlantic – Caribbean developing wave	WACDW	Wave developed a tropical depression over the West Atlantic or Caribbean longitude band
East Pacific developing wave	EPDW	Wave developed a tropical depression over the East Pacific longitude band
Nondeveloping wave	NDW	Wave never developed a tropical cyclone of at least tropical storm strength

948

949

950

951

952

953

954

955

956

957

958

959

960

961

962

963

964

965 TABLE 2. The number of distinct easterly waves and data points used for the trough composites
 966 of nondeveloping waves (NDWs), East Atlantic developing waves (EADWs), West Atlantic –
 967 Caribbean developing waves (WACDWs), and East Pacific developing waves (EPDWs). The
 968 numbers of distinct waves are valid over the full analysis domain (ALL) while the trough points
 969 are valid over individual longitude bands (bands defined as in Fig. 1). The asterisk indicates
 970 wave categories that are valid for July–August only. The number of individual NDWs is an
 971 estimate and includes an estimate of uncertainty because of the difficulty in counting these waves
 972 (see text). Finally, the missing values are for those composites that were unavailable.

	Sample Sizes					
	Distinct AEWs		Trough Points			
	ALL	EPC	CAR	WAT	EAT	AFR
NDW	330±40	2582	1695	1978	1737	2505
EADW	28	–	–	–	138	313
WACDW	37	–	102	290	317	436
EPDW*	68	267	358	361	287	392
NDW*	100±15	612	449	467	454	573

973

974

975

976

977

978

979

980

981

982

983

984

985 TABLE 3. The fractional coverage by IR brightness temperatures ≤ 240 K and ≤ 210 K for East
 986 Atlantic developing wave (EADW), West Atlantic – Caribbean developing wave (WACDW),
 987 and nondeveloping wave (NDW) phases valid over various longitude bands. The bold (italic)
 988 numbers indicate values that are significantly greater (less) than the corresponding NDW values
 989 valid at the 99% level.

IR Brightness Temperature Thresholds								
<i>Africa</i>								
	240 K				210 K			
	<i>Ridge</i>	<i>Northerly</i>	<i>Trough</i>	<i>Southerly</i>	<i>Ridge</i>	<i>Northerly</i>	<i>Trough</i>	<i>Southerly</i>
EADW	0.097	0.111	0.088	0.082	0.017	0.021	0.015	0.014
WACDW	0.068	0.085	0.083	0.079	0.013	0.017	0.015	0.013
NDW	0.061	0.073	0.071	0.065	0.010	0.014	0.013	0.010
<i>East Atlantic</i>								
	240 K				210 K			
	<i>Ridge</i>	<i>Northerly</i>	<i>Trough</i>	<i>Southerly</i>	<i>Ridge</i>	<i>Northerly</i>	<i>Trough</i>	<i>Southerly</i>
EADW	0.064	0.094	0.094	0.085	0.006	0.009	0.010	0.009
WACDW	0.046	0.064	0.086	0.069	0.004	0.004	0.008	0.005
NDW	0.072	0.059	0.075	0.088	0.005	0.004	0.006	0.007
<i>West Atlantic</i>								
	240 K				210 K			
	<i>Ridge</i>	<i>Northerly</i>	<i>Trough</i>	<i>Southerly</i>	<i>Ridge</i>	<i>Northerly</i>	<i>Trough</i>	<i>Southerly</i>
WACDW	0.077	0.067	0.103	0.110	0.007	0.008	0.011	0.015
NDW	0.062	0.045	0.056	0.068	0.005	0.004	0.005	0.006
<i>Caribbean</i>								
	240 K				210 K			
	<i>Ridge</i>	<i>Northerly</i>	<i>Trough</i>	<i>Southerly</i>	<i>Ridge</i>	<i>Northerly</i>	<i>Trough</i>	<i>Southerly</i>
WACDW	0.148	0.162	0.169	0.163	0.025	0.029	0.032	0.029
NDW	0.116	0.119	0.130	0.131	0.017	0.019	0.022	0.022

990

991

992

993

994

995

996 TABLE 4. Percentage convective coverage as a function of wave phase for East Atlantic
 997 developing waves (EADWs), West Atlantic – Caribbean developing waves (WACDWs), and
 998 nondeveloping waves (NDWs) valid over various longitude bands. The bold and italic values
 999 are as in Table 3.

Convective Coverage (%)				
<i>Africa</i>				
	<i>Ridge</i>	<i>Northerly</i>	<i>Trough</i>	<i>Southerly</i>
EADW	1.11	1.16	0.96	0.91
WACDW	0.74	0.91	0.86	0.89
NDW	0.78	0.76	0.80	0.78
<i>East Atlantic</i>				
	<i>Ridge</i>	<i>Northerly</i>	<i>Trough</i>	<i>Southerly</i>
EADW	0.98	1.48	1.41	1.18
WACDW	1.18	1.07	1.24	1.10
NDW	1.02	1.07	1.16	1.11
<i>West Atlantic</i>				
	<i>Ridge</i>	<i>Northerly</i>	<i>Trough</i>	<i>Southerly</i>
WACDW	1.44	1.42	1.70	1.59
NDW	1.25	1.33	1.43	1.46
<i>Caribbean</i>				
	<i>Ridge</i>	<i>Northerly</i>	<i>Trough</i>	<i>Southerly</i>
WACDW	1.77	2.03	1.76	1.81
NDW	1.70	1.66	1.78	1.73

1000
 1001
 1002
 1003
 1004
 1005
 1006
 1007
 1008
 1009

1010 TABLE 5. As in Table 4, except for lightning flash rates (flashes day⁻¹).

Lightning Flash Rates				
Africa				
	<i>Ridge</i>	<i>Northerly</i>	<i>Trough</i>	<i>Southerly</i>
EADW	179.2	133.2	109.0	153.8
WACDW	139.6	128.7	115.1	127.4
NDW	110.7	103.0	107.1	109.7
East Atlantic				
	<i>Ridge</i>	<i>Northerly</i>	<i>Trough</i>	<i>Southerly</i>
EADW	3.5	4.6	6.0	7.6
WACDW	1.0	3.3	5.0	6.1
NDW	2.4	3.0	4.4	8.5
West Atlantic				
	<i>Ridge</i>	<i>Northerly</i>	<i>Trough</i>	<i>Southerly</i>
WACDW	10.8	26.8	23.6	17.8
NDW	23.1	24.6	17.0	14.5
Caribbean				
	<i>Ridge</i>	<i>Northerly</i>	<i>Trough</i>	<i>Southerly</i>
WACDW	96.8	135.6	115.7	130.4
NDW	83.9	94.6	104.6	107.2

1011

1012

1013

1014

1015

1016

1017

1018

1019

1020

1021

1022

1023 TABLE 6. Mean polarization corrected temperatures at 37.0 and 85.5 GHz using 37.0-GHz
 1024 values ≤ 260 K and 85.5-GHz values ≤ 200 K (i.e., values associated with deep convection) for
 1025 East Atlantic developing wave (EADW), West Atlantic – Caribbean developing wave
 1026 (WACDW), and nondeveloping wave (NDW) phases valid over various longitude bands. No
 1027 EADW or WACDW values are significantly different from those of NDWs valid at the 99%
 1028 level.

Polarization Corrected Temperatures

Africa

	37.0				85.5			
	<i>Ridge</i>	<i>Northerly</i>	<i>Trough</i>	<i>Southerly</i>	<i>Ridge</i>	<i>Northerly</i>	<i>Trough</i>	<i>Southerly</i>
EADW	250.3	251.0	251.2	251.9	174.9	175.8	177.0	177.1
WACDW	251.5	252.2	251.6	251.6	175.1	176.0	176.3	176.1
NDW	251.4	251.7	251.7	251.7	176.4	176.4	177.0	177.7

East Atlantic

	37.0				85.5			
	<i>Ridge</i>	<i>Northerly</i>	<i>Trough</i>	<i>Southerly</i>	<i>Ridge</i>	<i>Northerly</i>	<i>Trough</i>	<i>Southerly</i>
EADW	257.4	256.4	256.5	256.1	185.9	184.0	184.3	183.0
WACDW	254.4	256.8	256.6	256.4	185.9	184.3	185.0	185.3
NDW	257.0	257.0	256.7	256.2	186.3	185.3	185.6	185.3

West Atlantic

	37.0				85.5			
	<i>Ridge</i>	<i>Northerly</i>	<i>Trough</i>	<i>Southerly</i>	<i>Ridge</i>	<i>Northerly</i>	<i>Trough</i>	<i>Southerly</i>
WACDW	255.8	254.5	255.2	255.5	183.7	181.5	183.5	182.2
NDW	255.3	254.7	255.3	255.6	183.0	182.0	183.1	183.4

Caribbean

	37.0				85.5			
	<i>Ridge</i>	<i>Northerly</i>	<i>Trough</i>	<i>Southerly</i>	<i>Ridge</i>	<i>Northerly</i>	<i>Trough</i>	<i>Southerly</i>
WACDW	255.5	252.6	253.2	253.3	181.0	177.5	177.4	178.4
NDW	253.7	253.5	253.3	253.2	178.0	178.6	178.6	178.5

1029

1030

1031

1032

1033

1034

1035 TABLE 7. The fractional coverage by IR brightness temperatures ≤ 240 K and ≤ 210 K, mean
 1036 polarization corrected temperatures (K) at 37.0 and 85.5 GHz using the same thresholds as in
 1037 Table 6, convective coverage (%), and lightning flash rates (flashes day⁻¹) for developing and
 1038 nondeveloping waves (30–50% Dev. and 30–50% ND, respectively) that were assigned a
 1039 30–50% probability of development within the next 48 hours by the National Hurricane Center.
 1040 Note that none of the 30–50% Dev. values are significantly different from the corresponding 30–
 1041 50% ND values valid at the 99% level.

IR Brightness Temperature Thresholds					
		<i>Ridge</i>	<i>Northerly</i>	<i>Trough</i>	<i>Southerly</i>
30-50% Dev.	240 K	0.108	0.115	0.154	0.172
	210 K	0.011	0.014	0.021	0.024
30-50% ND	240 K	0.104	0.079	0.133	0.125
	210 K	0.015	0.009	0.021	0.021

Polarization Corrected Temperatures					
		<i>Ridge</i>	<i>Northerly</i>	<i>Trough</i>	<i>Southerly</i>
30-50% Dev.	37.0	254.7	254.7	255.0	255.4
	85.5	185.4	182.1	182.2	183.0
30-50% ND	37.0	255.7	256.7	256.1	255.0
	85.5	180.1	183.1	183.6	180.6

Convective Coverage					
		<i>Ridge</i>	<i>Northerly</i>	<i>Trough</i>	<i>Southerly</i>
30-50% Dev.		1.56	1.48	1.93	1.93
30-50% ND		1.62	1.20	1.38	1.69

LIS Flash Rates					
		<i>Ridge</i>	<i>Northerly</i>	<i>Trough</i>	<i>Southerly</i>
30-50% Dev.		93.2	40.4	58.0	43.5
30-50% ND		38.3	8.2	10.5	89.1

1042

1043

1044

1045

1046 TABLE 8. The fractional coverage by IR brightness temperatures ≤ 240 K and ≤ 210 K for East
 1047 Pacific developing wave (EPDW) and nondeveloping wave (NDW) phases valid over various
 1048 longitude bands using only data valid for July and August. The bold and italic values are as in
 1049 Table 3.

IR Brightness Temperature Thresholds (July-August Only)

<i>Africa</i>								
240 K				210 K				
	<i>Ridge</i>	<i>Northerly</i>	<i>Trough</i>	<i>Southerly</i>	<i>Ridge</i>	<i>Northerly</i>	<i>Trough</i>	<i>Southerly</i>
EPDW	0.083	<i>0.100</i>	<i>0.093</i>	<i>0.068</i>	0.014	<i>0.017</i>	<i>0.016</i>	0.011
NDW	0.089	0.116	0.105	0.081	0.017	0.023	0.019	0.013
<i>East Atlantic</i>								
240 K				210 K				
	<i>Ridge</i>	<i>Northerly</i>	<i>Trough</i>	<i>Southerly</i>	<i>Ridge</i>	<i>Northerly</i>	<i>Trough</i>	<i>Southerly</i>
EPDW	0.054	0.048	0.057	0.049	0.004	0.003	0.004	0.002
NDW	0.048	0.052	0.064	0.053	0.003	0.003	0.005	0.004
<i>West Atlantic</i>								
240 K				210 K				
	<i>Ridge</i>	<i>Northerly</i>	<i>Trough</i>	<i>Southerly</i>	<i>Ridge</i>	<i>Northerly</i>	<i>Trough</i>	<i>Southerly</i>
EPDW	0.051	0.041	0.054	0.058	0.004	0.003	0.004	0.005
NDW	0.037	0.042	0.047	0.050	0.003	0.003	0.004	0.004
<i>Caribbean</i>								
240 K				210 K				
	<i>Ridge</i>	<i>Northerly</i>	<i>Trough</i>	<i>Southerly</i>	<i>Ridge</i>	<i>Northerly</i>	<i>Trough</i>	<i>Southerly</i>
EPDW	0.141	0.151	0.156	0.166	0.022	0.026	0.027	0.029
NDW	0.124	0.146	0.149	0.136	0.020	0.026	0.027	0.023
<i>East Pacific</i>								
240 K				210 K				
	<i>Ridge</i>	<i>Northerly</i>	<i>Trough</i>	<i>Southerly</i>	<i>Ridge</i>	<i>Northerly</i>	<i>Trough</i>	<i>Southerly</i>
EPDW	0.099	0.130	0.154	0.180	0.010	0.016	0.022	0.024
NDW	0.073	0.084	0.116	0.122	0.006	0.008	0.013	0.014

1050

1051

1052

1053

1054

1055

1056 TABLE 9. Lightning flash rates (flashes day⁻¹) for East Pacific developing wave (EPDW) and
 1057 nondeveloping wave (NDW) phases valid over various longitude bands using only data valid for
 1058 July and August. The bold and italic values are as in Table 3.

Lightning Flash Rates (July-August Only)				
<i>Africa</i>				
	<i>Ridge</i>	<i>Northerly</i>	<i>Trough</i>	<i>Southerly</i>
EPDW	123.6	131.6	138.4	109.6
NDW	206.7	143.8	142.4	120.8
<i>East Atlantic</i>				
	<i>Ridge</i>	<i>Northerly</i>	<i>Trough</i>	<i>Southerly</i>
EPDW	2.8	1.4	3.1	3.7
NDW	1.2	0.6	3.0	3.5
<i>West Atlantic</i>				
	<i>Ridge</i>	<i>Northerly</i>	<i>Trough</i>	<i>Southerly</i>
EPDW	12.1	14.2	19.8	16.2
NDW	8.2	16.6	14.8	17.4
<i>Caribbean</i>				
	<i>Ridge</i>	<i>Northerly</i>	<i>Trough</i>	<i>Southerly</i>
EPDW	104.8	138.3	137.4	115.5
NDW	112.0	161.1	126.1	119.6
<i>East Pacific</i>				
	<i>Ridge</i>	<i>Northerly</i>	<i>Trough</i>	<i>Southerly</i>
EPDW	58.5	68.2	72.8	69.5
NDW	18.9	32.2	37.0	36.4

1059

1060

1061

1062

1063

1064

1065

1066

1067

1068

1069 TABLE 10. A summary of the convective parameters that provide the greatest distinction
 1070 between nondeveloping waves and East Atlantic developing waves (EADWs), West Atlantic –
 1071 Caribbean developing waves (WACDWs), and East Pacific developing waves (EPDWs) over
 1072 various regions (EAT = East Atlantic, WAT = West Atlantic, CAR = Caribbean, and EPC = East
 1073 Pacific) in various phases. Suggested thresholds to initially be tested to determine the utility of
 1074 these parameters for tropical cyclogenesis forecasting are also provided. Note that the 240 K and
 1075 210 K IR coverage thresholds are nondimensional, while the flash rate threshold has units of
 1076 flashes day⁻¹.

Convective Parameters and Thresholds

<i>Wave Type</i>	<i>Location</i>	<i>Phase</i>	<i>Parameter</i>	<i>Threshold</i>
EADW	EAT	northerly/ trough	240 K IR coverage	0.090
EADW	EAT	northerly/ trough	210 K IR coverage	0.009
WACDW	WAT	southerly	240 K IR coverage	0.085
WACDW	WAT	southerly	210 K IR coverage	0.009
WACDW	CAR	trough	240 K IR coverage	0.155
WACDW	CAR	trough	210 K IR coverage	0.029
EPDW	CAR	southerly	240 K IR coverage	0.150
EPDW	EPC	trough/ southerly	240 K IR coverage	0.140
EPDW	EPC	northerly/ trough/ southerly	Flash rate	60.0

1077